

Cite this: *Chem. Commun.*, 2011, **47**, 7647–7649

www.rsc.org/chemcomm

COMMUNICATION

Differences in actinide metal–ligand orbital interactions: comparison of U(IV) and Pu(IV) β -ketoiminate N,O donor complexes[†]David D. Schnaars,^{ac} Enrique R. Batista,^{*b} Andrew J. Gaunt,^{*c} Trevor W. Hayton,^{*a} Iain May,^c Sean D. Reilly,^c Brian L. Scott^d and Guang Wu^a

Received 25th April 2011, Accepted 20th May 2011

DOI: 10.1039/c1cc12409a

Syntheses and characterization of $\text{UCl}_2(\text{Ar}^{\text{acnac}})_2$, $\text{UI}_2(\text{Ar}^{\text{acnac}})_2$, and $\text{PuI}_2(\text{Ar}^{\text{acnac}})_2$ are reported (Ar^{acnac} denotes a bis-phenyl β -ketoiminate ligand where $\text{Ar} = 3,5\text{-}^t\text{Bu}_2\text{C}_6\text{H}_3$). Structural analyses and computations show significant metal–ligand orbital interaction differences in U(IV) vs. Pu(IV) bonding.

Comparative bonding studies of molecular compounds across the actinide series are rare, with the exception of Th vs. U, which have long-lived low specific activity radioisotopes readily available for synthetic chemistry. For transuranic elements, significantly higher radiotoxicity hazards require specialized radiological facilities to allow safe manipulation.¹ Despite these practical challenges, establishing bonding trends and differences across the 5f series over a wide range of ligand types is important to provide underpinning chemical knowledge for nuclear fuel cycle applications.²

Historically, the majority of transuranic coordination chemistry reported is with hard O donor chelates for which ionic bonding to the metal is believed to be the only relevant consideration (the obvious exception being the terminal dioxo actinyl moieties which contain multiple bond character).³ Such donors were suitable for early actinide separation processes that utilized differences in actinide redox chemistry to access their markedly different chemical properties.³ However, advanced nuclear fuel cycles require alternative separations. For example, soft donors (N and S) are being studied for Am(III)/Cm(III) separation from the chemically similar Ln(III) ions by harnessing increases in An(III) vs. Ln(III) complex stability (likely due to subtle covalency increases).⁴ Here, we are interested in exploring subtle variations in 6d and 5f orbital interactions, which may

ultimately facilitate design of ligand sets for enhanced selective separations of actinides in the same oxidation state (e.g. An(IV)), and are of relevance to proposed group actinide extractions.⁵

β -Ketoiminate ligands have previously found utility in stabilizing $\text{U}^{\text{V}}\text{O}_2^+$ species through steric saturation of the equatorial plane.⁶ Their ability to form stable complexes with uranyl(V), a relatively weak Lewis acid, indicates that they should readily coordinate to An(IV) ions which are much stronger Lewis acids. We believe that Ar^{acnac} complexes are interesting candidates for comparison of U(IV) vs. Pu(IV) bonding parameters because they contain two different donor atoms within the same chelating ligand (O and N, respectively). These ligands would allow us to look for differences in metal–ligand interactions arising from 5f and 6d orbital participation. Our synthetic approach was to first demonstrate that β -ketoiminates can form stable U(IV) complexes and then attempt to isolate isostructural Pu(IV) complexes.

Treatment of 2 equivalents of the β -ketoiminate ligand $\text{Na}(\text{Ar}^{\text{acnac}})(\text{Ph})\text{CHC}(\text{Ph})\text{O}$ ($\text{Ar} = 3,5\text{-}^t\text{Bu}_2\text{C}_6\text{H}_3$) (generated *in situ*) with UCl_4 or $\text{UI}_4(\text{OEt}_2)_2$ forms $\text{UCl}_2(\text{Ar}^{\text{acnac}})_2$ (**1**) and $\text{UI}_2(\text{Ar}^{\text{acnac}})_2$ (**2**), respectively (Scheme 1). Preliminary attempts to synthesise the analogous Pu(IV) complexes, $\text{PuX}_2(\text{Ar}^{\text{acnac}})_2$ ($\text{X} = \text{Cl}$ or I), were complicated by the lack of readily accessible non-aqueous organic soluble Pu(IV) starting materials, with the only well established example being various salts of the $[\text{PuCl}_6]^{2-}$ anion.^{1,3} Reaction of $[\text{PPh}_4][\text{PuCl}_6]$ with two equivalents of $\text{Na}(\text{Ar}^{\text{acnac}})$ did not lead to isolation of $\text{PuCl}_2(\text{Ar}^{\text{acnac}})_2$.⁷ As an alternative strategy, the use of Pu^0 as a precursor to a low valent Pu β -ketoiminate complex was examined. We initially employed reaction conditions designed to isolate a Pu(III) complex because prior observations had suggested that direct oxidation to Pu(IV) was unlikely (excess I_2 or Br_2 alone does not oxidize Pu^0 to Pu^{IV} under inert atmospheric/anhydrous conditions).⁸ However, oxidation of

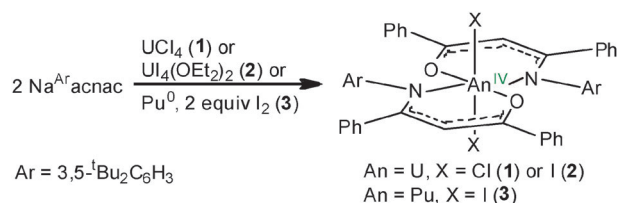
^a Department of Chemistry and Biochemistry, University of California Santa Barbara, Santa Barbara, CA 93106, USA. E-mail: hayton@chem.ucsb.edu; Tel: +1 805 893 3392

^b Theoretical Division, Los Alamos National Laboratory, Los Alamos, NM 87545, USA. E-mail: erb@lanl.gov; Tel: +1 505 667 8177

^c Chemistry Division, Los Alamos National Laboratory, Los Alamos, NM 87545, USA. E-mail: gaunt@lanl.gov; Tel: +1 505 667 3395

^d Materials Physics and Applications Division, Los Alamos National Laboratory, Los Alamos, NM 87545, USA

[†] Electronic supplementary information (ESI) available: Syntheses of **1–3**, IR, NMR, UV/vis/nIR, cyclic voltammetry, DFT calculation details, and CIF's for **1–3**. CCDC 824025–824027. For ESI and crystallographic data in CIF or other electronic format see DOI: 10.1039/c1cc12409a



Scheme 1 General preparative routes to **1–3**.

Pu^{IV} with 1.6 equivalents of I_2 in THF followed by treatment with 2 equivalents of $\text{Na}(\text{Ar}^{\text{acnac}})$ (*in situ*) afforded several single crystals of $\text{Pu}^{\text{IV}}\text{I}_2(\text{Ar}^{\text{acnac}})_2$, rather than the anticipated $\text{Pu}(\text{III})$ complex.⁹ In light of this surprising result we increased the initial stoichiometry of I_2 to two equivalents providing isolation of $\text{Pu}^{\text{IV}}\text{I}_2(\text{Ar}^{\text{acnac}})_2$ (**3**) in a low, but pure (single crystals), 17% yield (Scheme 1). It is likely that access to the $\text{Pu}(\text{IV})$ oxidation state is made possible by the strong electron donating ability of the Ar^{acnac} ligand shifting the $\text{Pu}(\text{III})/\text{Pu}(\text{IV})$ redox potential within the range of I_2 .

The ^1H NMR spectra of **1–3** exhibit paramagnetic shifting and contain resonances consistent with the formulation of the proposed complexes (Fig. S6–8†). Interestingly, the addition of 1 equiv of THF to a C_6D_6 solution of **1** results in a change of the resonance profile, suggesting possible coordination to the complex (Fig. S6A–B†). Additionally, in the ^1H NMR spectrum of **2** in CD_2Cl_2 , the broad resonances at -1.10 ppm and -3.84 ppm are consistently present (independent of the synthetic method) and we have tentatively assigned them as the two inequivalent ^tBu environments arising from the presence of a minor *cis* isomer (Fig. S7†).

In the solid state, **1–3** are geometrically isostructural consisting of a six coordinate $\text{An}(\text{IV})$ metal centre with a ligand arrangement best described as distorted octahedral (Fig. 1, S3–5†). In each case, the halides sit *trans* to one another in axial positions and the two bidentate Ar^{acnac} ligands occupy the equatorial plane in a *trans* configuration. In addition to being geometrically isostructural, the bond lengths and angles between uranium and the Ar^{acnac} ligand in **1** and **2** are identical within statistical errors (Table 1), thus the identity of the coordinated halide has no significant effect upon the metrical parameters associated with the coordination of the Ar^{acnac} ligand to uranium.

The structural similarity of **2** to **3** offers a very rare opportunity for a direct comparison of $\text{U}(\text{IV})$ vs. $\text{Pu}(\text{IV})$ solid state molecular structures (Table 1). Firstly, considering the An–I bonding, the U–I distance in **2** is $3.0288(5)$ Å, whilst the Pu–I distance in **3** is 0.043 Å shorter, with a length of $2.9859(3)$ Å. This represents the first example of a $\text{Pu}(\text{IV})\text{–I}$ bond. Secondly, considering the An–N bonding to the Ar^{acnac} ligand, the U–N distance in **2** is $2.409(5)$ Å and the Pu–N distance in **3** is $2.3635(19)$ Å. As expected from the actinide contraction and increasing effective positive charge of the $\text{An}(\text{IV})$ ions across the series, the Pu–N bond is shorter than the U–N bond,

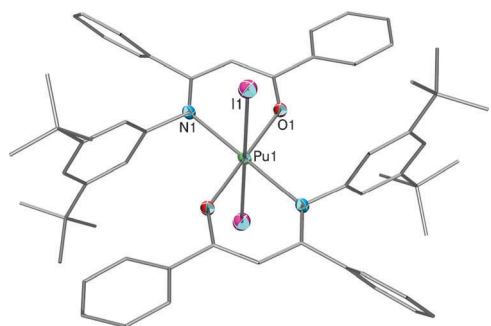


Fig. 1 Solid-state structure of **3** with 50% probability ellipsoids. H atoms and solvent have been omitted for clarity. **1** and **2** are geometrically isostructural. Lattice solvation also differs between **1–3**.

although the difference of 0.046 Å is perhaps slightly larger than might be anticipated (the ionic radii for the 6-coordinate metal ions differ by 0.03 Å; 0.89 Å for U and 0.86 Å for Pu).¹⁰ Thirdly, considering the An–O bonding to the Ar^{acnac} ligand, the U–O distance in **2** is $2.163(4)$ Å and the Pu–O distance in **3** is $2.1727(17)$ Å. These bonds differ by just 0.01 Å, are within statistical error of each other, and thus do not follow the expected trend of a similar shortening of the U–O vs. Pu–O bond in the way that the U–N vs. Pu–N bond shortens. The fact that the O and N donor atoms in **2** and **3** are contained within the same ligand (Ar^{acnac}), yet do not exhibit similar changes in bond lengths upon moving from $\text{U}(\text{IV})$ to $\text{Pu}(\text{IV})$ (*i.e.* An–O remains the same while An–N shortens), suggests that the bonding changes in these complexes across the $\text{An}(\text{IV})$ series are not adequately explained by the actinide contraction and ionic bonding models alone.

The only other $\text{U}(\text{IV})/\text{Pu}(\text{IV})$ discrete molecular isostructural comparison that we are aware of in the literature is the polyoxometalate anion $[\text{An}(\alpha_2\text{-P}_2\text{W}_{17}\text{O}_{61})_2]^{16-}$ ($\text{An} = \text{Th}, \text{U}, \text{Np}, \text{Pu}, \text{Am}$), which afforded an isostructural comparison of An–O bonds across the $\text{An}(\text{IV})$ series.¹¹ In that study, the average Pu–O distance is shorter than the average U–O distance by 0.03 Å, and was attributed to the effect of the different ionic radii of the 8-coordinate metal centres (1.00 Å for U and 0.96 Å for Pu).¹⁰ The scarcity of literature comparisons and the unexplained bond length trends in **2** and **3** motivated us to probe the metal–ligand interactions further.

We turned to hybrid DFT modeling, demonstrating reasonable agreement between the experimental and calculated structures, and although actinide–ligand bond distances tend to be overestimated by DFT,¹² the larger variation in the An–N (0.04 Å) distances vs. the An–O distances (0.01 Å) between **2** and **3** is accurately captured (Table 1). Natural orbital analysis indicates a clean unpaired spin density with ground state configurations triplet $\text{U}(5f^2)$ for **2** and quintet $\text{Pu}(5f^4)$ for **3** (Fig. S17–18†). Further $5f$ and $6d$ electronic density from the U and Pu (0.7 and $1 e^-$, respectively) is involved in bonding interactions with the I, O, and N ligands. Natural orbitals indicate the $5f$ density is involved in three σ -type bonds between U or Pu and the three ligand types. The $6d$ density participates in σ bonding with the I and π bonding with the O and N atoms, however, it is challenging to deconvolute all three interactions as the ligands interact with one another. We then performed a Natural Bond Orbital (NBO) analysis. The metal was identified as a fragment by itself in both **2** and **3** and so was the iodine, while the oxygen and nitrogen fragments are represented as core and lone-pair orbitals (LP) plus bonding orbitals with the neighboring carbon. The level of interaction and energy stabilization *via* charge transfer from occupied natural atomic orbitals was obtained by second order perturbation analysis in that basis (Table S2–3†). The largest interaction corresponds to dative bonds from the occupied oxygen and nitrogen lone pairs to the virtual lone pairs of the metal (Fig. S19–24† show all LPs).

For the An–N interactions, the overall strength is very similar for $\text{U}(\text{IV})$ vs. $\text{Pu}(\text{IV})$ and there are two main contributions in both cases: in the Pu complex (**3**) the stabilization energies are 21 and 7 kcal mol⁻¹, and in the U complex (**2**) they are 25 and 8 kcal/mol. In both cases the interacting

Table 1 Selected bond distances (Å) and angles (°) for **1–3**

	1	2	3	Calculated	
	M = U, X = Cl	M = U, X = I	M = Pu, X = I	2	3
M–X	2.6315 (12)	3.0288 (5)	2.9859 (3)	3.073	3.045
M–O	2.173 (3)	2.163 (4)	2.1727 (17)	2.185	2.198
M–N	2.406 (3)	2.409 (5)	2.3635 (19)	2.462	2.422
X–M–X	180	180	180	180	180
O–M–N	71.19 (11)	71.06 (15)	73.29 (7)	72.67	75.58

orbitals are almost the same: the N lone pair (25% s + 75% p) couples with a 100% 5f orbital in the smaller contribution, and in the larger contribution the N lone pair couples with a metal virtual LP of 6d and 7s orbital composition. Analysis of the An–O interactions indicates that the U–O orbital interactions are stronger than the Pu–O orbital interactions. In contrast to the An–N interactions, the interacting pairs in the An–O bonds are different between **2** and **3** (see Fig. 2 for representations of the strongest An–O interactions in **2** and **3**). Three dominating pairs are found in the U–O bond: the first of energy 23 kcal mol⁻¹ involving the LP1 in oxygen (40% s + 60% p) and a virtual LP in the U (70% 6d + 30% 7s), the second of energy 15 kcal mol⁻¹ involving the LP2 in oxygen (16% s + 84% p) and the same virtual LP in U, and the third of energy 13 kcal mol⁻¹ involving the LP2 in oxygen and a virtual LP in U (100% 5f). There are another three minor interactions of 5.5, 4.7 and 4.3 kcal mol⁻¹ for the U–O bond. Turning to the Pu–O bond, there is one main interaction of 16.5 kcal mol⁻¹ between LP1 of the oxygen (46% s + 54% p) and a 100% 6d orbital of Pu. The rest of the Pu–O interaction comprises four minor contributions of 8.9, 6.5, 5.7, and 5.4 kcal mol⁻¹ all involving the same oxygen LP2 (12% s + 88% p) with a 100% 6d orbital, a 100% 5f_π, a 52% 6d + 48% 7s orbital, and a 100% 5f_φ orbital, respectively. A fifth minor interaction of 6.1 kcal mol⁻¹ is between the oxygen LP3 (100% p) and a 100% 6d LP in Pu.

We interpret the increased sum of the orbital interactions for the U–O bond (65.5 kcal mol⁻¹) vs. the Pu–O bond (49.1 kcal mol⁻¹) as an explanation for the observed shortening of the U–O bond with respect to the Pu–O bond. Since the U–N vs. Pu–N interaction compositions and total strength (33 and 28 kcal mol⁻¹, respectively) are similar, we attribute the experimentally observed shorter Pu–N vs. U–N bond to the effect of

the actinide contraction. This finding is significant because, upon considering the role of covalency in f-element separations, it is usually the softer donors (N or S atoms) which are anticipated to exhibit differences that can result in selectivity for a particular actinide ion. NBO analysis of the relative charges on the O vs. N atom in **2** and **3** confirm that the O atom is ‘harder’ than the N atom in the ^{Ac}racnac ligand (–0.744 and –0.757 on O in **2** and **3**, compared to –0.617 and –0.632 on N; about 17% smaller) and yet it is this ‘hard’ oxygen donor which is the origin of metal–ligand orbital overlap differences rather than the relatively ‘soft’ N atom. However, further comparisons of isostructural O-donor actinide complexes are required to facilitate development of how these bonding differences can be exploited in ligand designs for advanced nuclear fuel cycle separation processes.

We thank the University of California, Santa Barbara, and the University of California Laboratory Fees Program. D.D.S. thanks the Seaborg Institute Summer Research Fellowship Program at LANL. A.J.G./S.D.R. thank the U.S. Department of Energy, Office of Science, Early Career Research Program (contract DE-AC52-06NA25396). E.R.B./I.M. thank the U.S. Department of Energy, Office of Science, Basic Energy Sciences, Heavy Element Chemistry Research Program.

Notes and references

- 1 A. J. Gaunt and M. P. Neu, *C. R. Chim.*, 2010, **13**, 821.
- 2 Spent fuel reprocessing options, IAEA-TECDOC-1587, 2008, http://www-pub.iaea.org/MTCD/publications/PDF/te_1587_web.pdf.
- 3 *The Chemistry of the Actinide and Transactinide Elements*, ed. L. R. Morss, N. M. Edelstein, J. Fuger and J. J. Katz, Springer, Dordrecht, The Netherlands, 2006.
- 4 See, for example (and references therein): A. J. Gaunt, S. D. Reilly, A. E. Enriquez, B. L. Scott, J. A. Ibers, P. Sekar, K. I. M. Ingram, N. Kaltsoyannis and M. P. Neu, *Inorg. Chem.*, 2008, **47**, 29; M. P. Jensen and A. H. Bond, *J. Am. Chem. Soc.*, 2002, **124**, 9870.
- 5 E. Aneheim, C. Ekberg, A. Fermvik, M. R. S. Foreman, T. Retegan and G. Skarnemark, *Solvent Extr. Ion Exch.*, 2010, **28**, 437.
- 6 T. W. Hayton and G. Wu, *Inorg. Chem.*, 2009, **48**, 3065.
- 7 Method of synthesis of [PPh₄]₂[PuCl₆] provided by S. A. Kozimor, *et al.*, and is to be reported elsewhere.
- 8 A. J. Gaunt, S. D. Reilly, A. E. Enriquez, T. W. Hayton, J. M. Boncella, B. L. Scott and M. P. Neu, *Inorg. Chem.*, 2008, **47**, 8412.
- 9 X-ray structural data was low quality but clearly established atom identities and molecular connectivity.
- 10 R. D. Shannon, *Acta Crystallogr., Sect. A: Cryst. Phys., Diffr., Theor. Gen. Crystallogr.*, 1976, **32**, 751.
- 11 M. N. Sokolova, A. M. Fedosseev, G. B. Andreev, N. A. Budantseva, A. B. Yusov and P. Moisy, *Inorg. Chem.*, 2009, **48**, 9185.
- 12 T. W. Hayton, J. M. Boncella, B. L. Scott, E. R. Batista and P. J. Hay, *J. Am. Chem. Soc.*, 2006, **128**, 10549.

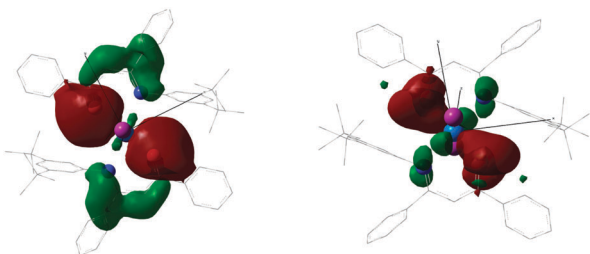


Fig. 2 The strongest An–O orbital interaction in **2** compared to **3**: a 23 kcal mol⁻¹ U–O couple with 30% 7s and 70% 6d character for the metal contribution (left), and a 16.5 kcal mol⁻¹ Pu–O couple with 100% 6d character for the metal contribution (right).